Review Article **Open Access**

Prineha Narang, Ravishankar Sundararaman, and Harry A. Atwater

Plasmonic hot carrier dynamics in solid-state and chemical systems for energy conversion

DOI: 10.1515/nanoph-2016-0007
Received October 22, 2015; accepted January 14, 2016

Abstract: Surface plasmons provide a pathway to efficiently absorb and confine light in metallic nanostructures, thereby bridging photonics to the nano scale. The decay of surface plasmons generates energetic 'hot' carriers, which can drive chemical reactions or be injected into semiconductors for nano-scale photochemical or photovoltaic energy conversion. Novel plasmonic hot carrier devices and architectures continue to be demonstrated, but the complexity of the underlying processes make a complete microscopic understanding of all the mechanisms and design considerations for such devices extremely challenging. Here, we review the theoretical and computational efforts to understand and model plasmonic hot carrier devices. We split the problem into three steps: hot carrier generation, transport and collection, and review theoretical approaches with the appropriate level of detail for each step along with their predictions. We identify the key advances necessary to complete the microscopic mechanistic picture and facilitate the design of the next generation of devices and materials for plasmonic energy conversion.

1 Introduction

Surface plasmons are collective oscillations of electrons in conductors coupled to electromagnetic modes that are confined to conductor–dielectric interfaces [1–4]. They enable efficient coupling of electromagnetic waves from free space to nanoscale systems [5–9], and have therefore found a broad range of applications, including spectroscopy, non-linear optics [10, 11], photodetection [12–15], and solar energy harvesting [16, 17]. Additionally, novel phenomena continue to be discovered in the field of plasmonics, such as quantum interference of plasmons [18–20], quantum coupling of plasmons to single-particle excitations, and quantum confinement of plasmons in single-nm scale plasmonic particles [21–23]. Experimental developments in quantum plasmonics have shown, remarkably, the ability of surface plasmons to preserve many key quantum mechanical properties of the photons used to excite them, notably entanglement, interferometry and sub-Poissonian statistics.

Surface plasmons provide high-mode confinement because the electric field substantially penetrates into the metal, but this also increases losses. This trade-off between localization and loss has hampered widespread applications of plasmonic waveguides and nano resonators for applications in integrated photonics. However, losses in plasmonics also provide unique opportunities. For example, the short dephasing times can be used to enhance the emission of nearby nanoemitters with lower internal quantum efficiency [24–26]. Additionally, the decay of surface plasmons creates electron–hole pairs with energies much larger than those in the background thermal distribution, and these 'hot' carriers enable processes not possible with thermalized carriers.

Plasmonic hot carriers provide tremendous opportunities for combining efficient light capture with energy conversion and catalysis at the nano scale. The hot carriers could be used to directly drive chemical reactions at the metal surface [27], or they could be transferred to a semiconductor for use in photovoltaics [28–30] and photoelectrochemical systems [31–33]. Composite systems allow combining traditional carrier generation in semiconductors with enhanced sub-band-gap absorption in metallic nanoparticles and injection of the generated carriers into the semiconductor, for additional light harvesting. Plasmonic systems can potentially also be used to tailor carrier energy distributions as well as localize them spatially and temporally in order to exert tremendous control on the photocatalytic processes, possibly even for selectivity. Plasmon-enhanced energy conversion devices, such as for water splitting, have been demonstrated using composite metal–semiconductor photocatalysts as well as all-in-one catalytic noble metal plasmonic nanostructures [34–43]. The significant experimental effort in plasmonic hot

Prineha Narang, Ravishankar Sundararaman, Harry A. Atwater: Joint Center for Artificial Photosynthesis, California Institute of Technology, Pasadena CA 91125 USA
Prineha Narang, Harry A. Atwater: Thomas J. Watson Laboratories of Applied Physics, California Institute of Technology, Pasadena CA 91125 USA

carrier–driven processes and devices has been the focus of several recent reviews [44–46]. This review emphasizes an overall theoretical understanding of the microscopic mechanisms underlying, and thereby the fundamental limits of, plasmon decay to hot carriers and their utilization for energy conversion.

The microscopic mechanisms in plasmon decays across various energy, length, and time scales are still a subject of considerable debate, as seen in recent experimental and theoretical papers [47–49]. A great majority of investigations of plasmonic nanostructures focus on their optical response, usually described adequately within classical electromagnetic theory [3]. However, quantum effects become important in the single photon limit since plasmons are fundamentally quantum mechanical [21, 50], as well as in small nanostructures due to carrier confinement, tunneling, and uncertainty principle effects. The quantum effects on carriers are adequately described by time-dependent density functional theory (TDDFT) [51, 52] in the jellium approximation (which simplifies the band structure to a free-electron one), for example, tunneling effects in nanoparticle dimers [53–56]. First-principles calculations that retain the full electronic band structure are necessary in order to capture effects beyond the free electron limit, for example, anisotropy of surface plasmon response on noble metal surfaces [57]. More importantly, such calculations are critical for describing all the mechanisms of plasmon decay and gauging their relative contributions. Such calculations are currently feasible for nanoparticles containing up to a few hundred atoms, that is, 1–2 nm in size, and can explicitly account for the effects of nanoparticle shape with specific facets and surface states on the optical response and carrier generation [58–60].

A complete theoretical investigation of real plasmonic hot carrier based energy conversion devices is, however, extremely challenging. The optical response of these devices depends on length scales ranging from a few nanometers to hundreds of nanometers or microns, and this presents challenges even for classical electromagnetic simulations. On the other hand, carrier generation requires a quantum mechanical electronic structure treatment where the relevant length scales are in Angstroms, and the current practical upper limit for such theories is a few nanometers. Figure 1 illustrates this disparity in length scales, and also points out the disparate time scales ranging from carrier thermalization by electron–electron scattering tens of femtoseconds after excitation, to equilibration with lattice by electron–phonon scattering picoseconds later.

A single level of theory cannot adequately describe plasmonic hot carrier devices spanning all the relevant length and time scales discussed above, and this necessitates a multi-scale, multi-paradigm description. Figure 2 outlines the separation of a plasmonic energy conversion device (either photovoltaic or photocatalytic) into steps that can each be described at a different appropriate level of theory. The coupling of light from free space to surface plasmons can be treated using classical electromagnetic theory, and we do not deal with that well-studied aspect here. Section 2 describes the decay of surface plasmons to generate carriers in the material using a combination of jellium and first-principles electronic structure methods. Section 3 then discusses the dynamics of the generated carriers, including electron–electron and electron–phonon scattering described using electronic structure methods, and their transport in plasmonic nanostructures. Finally, section 4 deals with injection of the carriers into molecules at the surface or across metal–semiconductor Schottky barriers, and describes the necessary theoretical considerations in each case.

2 Hot carrier generation from plasmon decay

Surface plasmons can decay either radiatively [14, 61], by emitting a photon, or nonradiatively, by single-particle electronic excitations [62] that generate non-thermal electrons and holes, typically referred to as hot carriers. For plasmons, the collective excitations of electrons in metals, this decay to single-particle excitations constitutes Landau damping. Several microscopic mechanisms contribute to the Landau damping of plasmons, and their relative importance depends on the material, plasmon energy, and geometry.

Photons and surface plasmons have negligible momenta compared to the crystal momenta of electrons. In bulk materials, this implies that direct decay of plasmons can only create electron–hole pairs with net zero crystal momentum, and such pairs of electronic states are only available in the band structure of most metals above a certain interband threshold energy. Below this interband threshold, absorption or emission of phonons accompanies the plasmon decay to provide the necessary momentum to excite electrons to states with different crystal momenta. Figure 2 shows the Feynman diagrams corresponding to direct and phonon-assisted decay of surface plasmons. Note that we do not distinguish carrier excitations due to surface plasmons from those due to photons be-

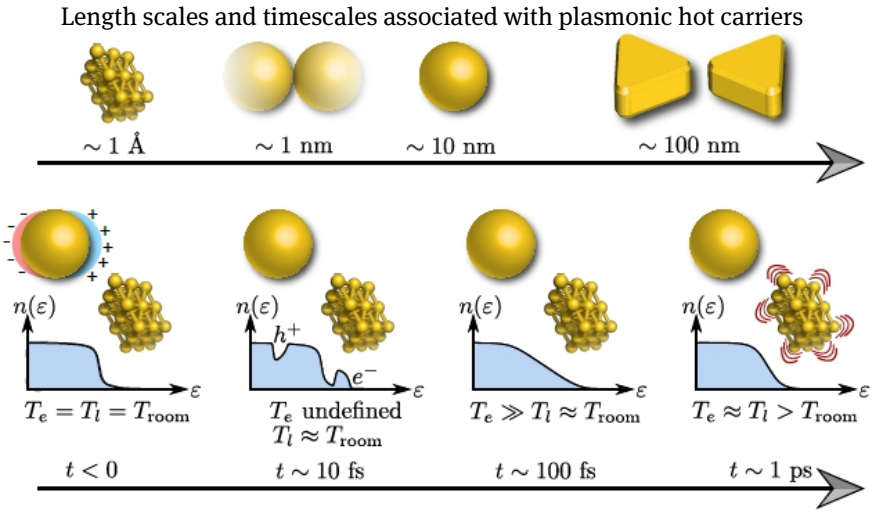

Fig. 1. Top panel: length scales in plasmonics vary from the atomic to the mesoscale. Shown from left to right: atomic lattice, small gaps in nanoparticle dimers, nanoparticles and bowtie antennae. Lower panel: typical time scales for the the excitation of hot carriers and their subsequent relaxation. In the 10 fs regime, carrier distributions do not resemble Fermi distributions at any temperature, but at later times the dynamics can be described approximately by distinct electron and lattice temperatures, T_e and T_l.

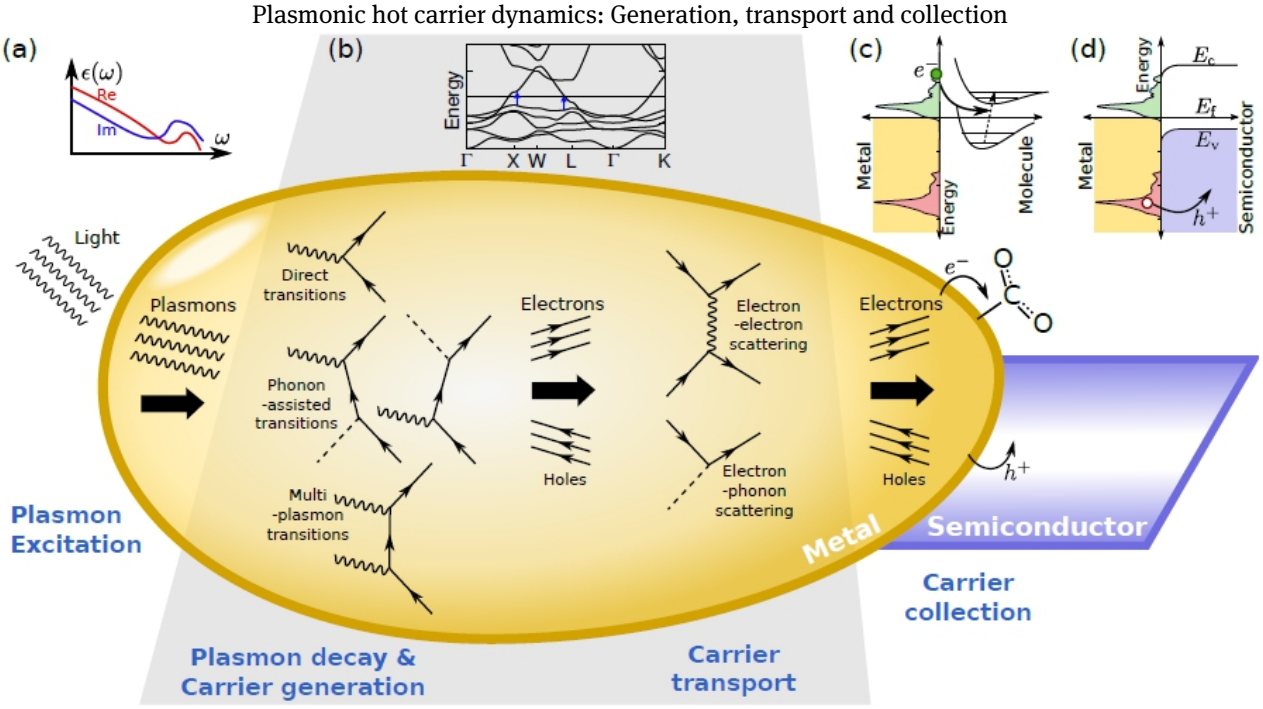

Fig. 2. Processes involved in the excitation of plasmons, their decay to hot carriers, the transport of hot carriers in plasmonic nanostructures and their collection either in adsorbed molecules or semiconductors (lower part). The top part of the figure shows the theoretical methods with a level of detail appropriate for each stage: (a) dielectric functions for plasmon excitation (b) electronic structure theory for carrier generation and transport, and (c) band / energy-level alignment analysis for collection. Feynman diagrams indicate the relevant processes at each stage: direct transitions, phonon-assisted transitions, and multiplasmon decay (in the high-intensity range only) for generation, and electron-electron and electron–phonon scattering for transport. Collection of hot carriers in solid-state systems can be used for solar energy conversion devices, sensitive photodetectors, and nano-spectrometers. Hot carriers injected into molecules on a surface can induce photochemical reactions, for example, CO_2 reduction, which is mechanistically very different from solid state collection.

cause carrier generation only depends on the net electric field distribution in the metal. This field distribution consists of a superposition of photon and surface plasmon modes for an illuminated metal nanostructure, depending on the frequency of illumination relative to the plasmon resonance. We therefore separate the questions of carrier generation, which focuses on microscopic mechanisms such as direct and phonon-assisted excitations, from the question of field distributions, which can be obtained from classical electromagnetic simulations accounting for photonic and plasmonic contributions.

In nanoscale systems, the electronic states are localized in space and are therefore no longer exact (crystal) momentum eigenstates by the uncertainty principle. This introduces a finite probability of direct plasmon decay into an electron–hole pair with net crystal momentum, which can occur even for plasmons below the interband threshold energy. For definiteness, we refer to these as geometry-assisted intraband transitions because the nano-scale geometry provides the momentum in lieu of phonons to induce the transitions within the conduction band of the metal. Some distinguish this process as plasmon-induced carrier generation in contrast to direct and phonon-assisted transitions as photoexcited carrier generation [49], but we emphasize that the key difference is in the localized electronic states; optical excitation far from the plasmonic resonance will also induce geometry-assisted transitions in small nanoparticles.

A complete understanding of plasmonic hot carrier generation requires accounting for material as well as geometry effects. The decay mechanisms in bulk materials, direct and phonon-assisted transitions, are strongly dependent on the electronic band structure of the metal, whereas the geometry-assisted transitions occur predominantly in the free-electron like conduction band. Theoretically, the former require detailed bulk electronic structure calculations, whereas the latter can be treated using free-electron-like jellium models but require explicit inclusion of geometry in the quantum mechanical method. Different theoretical approaches spanning different levels of detail and system size have been applied to different aspects of hot carrier generation, and we need a combination of these to understand the relative contributions of all mechanisms as a function of material, energy, and geometry.

2.1 Geometry dependence: intraband transitions

In nano-scale metallic systems, the free-electron-like conduction band splits into several discrete states with non-zero matrix elements for optical transition between them (they are zero within the band for the bulk metal). This is a consequence of the geometry breaking translation invariance so that the Hamiltonian no longer commutes with crystal momentum and the energy eigenstates do not have definite crystal momentum.

Theoretical calculations can capture this effect by solving the Schrödinger equation for electronic states in the actual geometry, and using Fermi's Golden rule with optical matrix elements between these states to calculate the transition rate induced by the plasmon. The level of detail in the electronic states vary from analytical free-electron solutions [48, 63, 65], jellium time-dependent density functional theory (TD-DFT), which neglects atomic-scale structure in the nuclear potential and therefore details in the band structure but approximately accounts for electron–electron interactions [64], to TD-DFT calculations with full band-structure for small metal clusters [59]. The full calculations are currently feasible only for clusters with very few atoms (2–3 nm across), whereas the free electron and jellium TD-DFT calculations can be extended to $\sim$ 20 nm nanoparticles and they yield qualitatively similar results [64].

Figure 3(a) shows the predicted initial energy distribution of hot carriers generated due to geometry-assisted intraband transitions in gold nano-platelets [63]. These transitions predominantly generate low-energy electrons near the Fermi level for larger particles $\sim$ 40 nm, whereas produce continuous distributions of electrons extending from the Fermi energy to the plasmon energy above it for very small particles $\lesssim$ 10 nm. Figure 3(b) shows a similar dependence of the carrier generation in spherical nanoparticles of various sizes [64]. It additionally shows that the net hot carrier rate decreases with carrier lifetime, by incorporating lifetime as a Lorentzian broadening in Fermi's golden rule. (We contrast this rudimentary treatment of transport effects with more complete models below in Section 3.)

The free electron / jellium approaches are invaluable in treating geometry-assisted plasmon decay in experimentally relevant structures, but they are sufficient only for materials and ranges of plasmon energies that only involve the free-electron-like conduction band, and where the other decay mechanisms are negligible. This is reasonably valid for silver below its interband threshold of 3.6 eV, which is what most of these studies focus on, but less applicable to gold and copper, which exhibit direct transitions at lower energies $\sim$ 2 eV, and inapplicable to aluminum, which undergoes direct transitions at all energies. We additionally need to include the material-dependent direct and phonon-assisted processes, which in turn re-

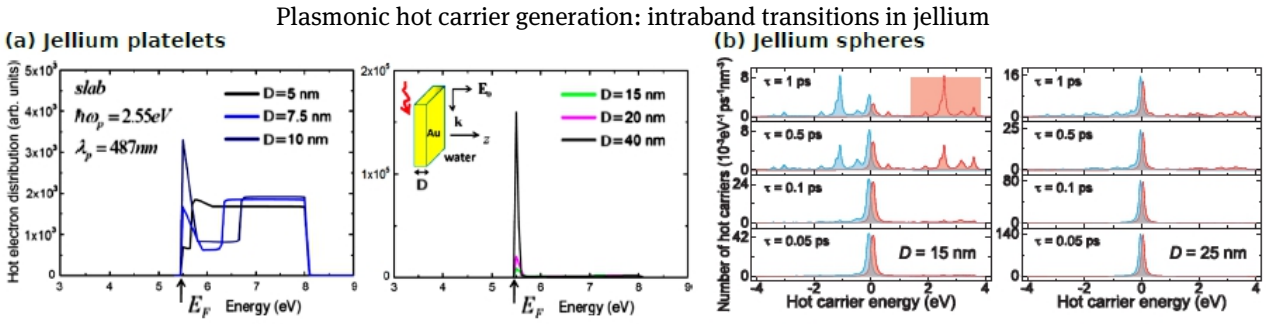

Fig. 3. Initial hot carrier energy distributions due to geometry-assisted intraband transitions in (a) gold platelets [63] and (b) silver spheres [64] using a jellium (free electron) approach. Part (b) additionally incorporates an energy-independent carrier lifetime τ as a Lorentzian broadening in Fermi's golden rule. The probability of high-energy electrons and holes decreases sharply as τ decreases or the dimension D increases. Part (a) adapted from Ref. 63 and part (b) from Ref. 64 (© 2013 and 2014 respectively, American Chemical Society).

quire a more detailed treatment that fully accounts for the electronic band structure.

2.2 Material dependence: direct and phonon-assisted transitions

Electronic structure methods including density-functional theory (DFT) and many-body perturbation theory within the GW approximation can predict accurate electronic band structures and optical matrix elements for the bulk material. Recently, the decay of surface plasmons via direct transitions in the bulk material has been examined in detail using Fermi's golden rule calculations on relativistic DFT+U band structures [66], and confirmed by subsequent GW calculations [68].

Figure 4 shows the theoretical predictions for the carrier distributions generated by direct transitions in several plasmonic metals, and annotates the dominant transitions on the band structures of the metals [66]. Direct transitions are very sensitive to the band structure because of the selection rule that requires initial and final electronic states with equal crystal momentum. In copper and gold, these transitions are predominantly from the d-bands deep below the Fermi level to the conduction band, which results in high-energy holes and lower energy electrons, whereas in silver, transitions from the conduction band can additionally produce high-energy electrons with lower energy holes. Aluminum produces a continuous energy distributions of electrons as well as holes ranging from zero to the plasmon energy. Additionally, this selection rule also results in strongly anisotropic initial momentum distributions dominated by the crystal directions (rather than the polarization direction) for noble metals, as shown in the bottom panels of Figure 4. The polarization direction controls the carrier momentum distribution only in aluminum because of the band crossing near the Fermi level [66].

Ab initio electronic structure calculations have recently also become feasible for phonon-assisted transitions and have been used to study the optical properties of indirect bandgap semiconductors [69, 70]. Subsequently, this approach has been generalized to metals, which requires additional careful treatment of singular contributions from sequential processes, and applied to the study of plasmon decay [67]. These calculations show that phonon-assisted transitions also generate uniform electron and hole energy distributions ranging from zero to the plasmon energy, similar to geometry-assisted transitions.

Most importantly, accounting for direct and phonon-assisted transitions, along with resistive losses at lower frequencies, *quantitatively* accounts for the experimental absorption in metals from mid-IR to UV frequencies as shown for gold in Figure 5(a) [67]. Combined with jellium estimates for geometry-assisted transitions in spherical nanoparticles, this also enables estimating the relative contributions of bulk and geometry-dependent decay for particles of various sizes, as shown in Figure 5(b-c) [67]. Direct transitions dominate above the interband threshold even for very small particles $\sim$ 10 nm, whereas phonon-assisted and geometry-assisted intraband transitions compete below threshold. These two intraband transitions contribute approximately equally for 40 nm particles, and the relative importance of the geometry-assisted transitions varies inversely with particle diameter.

This combination of *ab initio* electronic structure methods for detailed material properties with free electron / jellium calculations for nano-scale geometry enables understanding the relative contributions of different plasmon decay mechanisms and predicting the initial energy distribution of hot carriers thus generated. Such calcula-

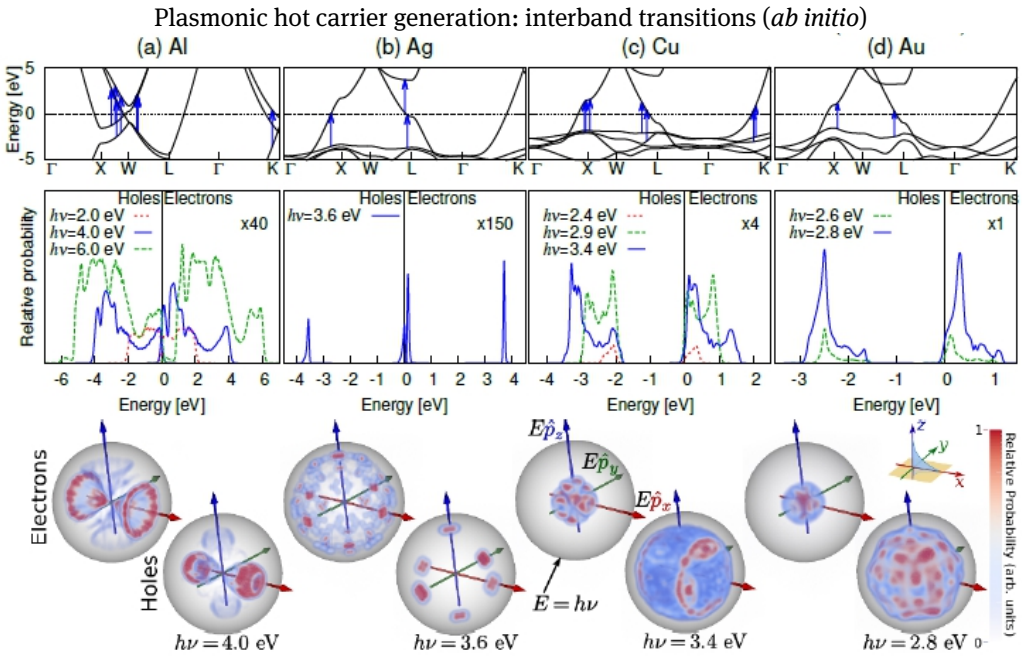

Fig. 4. Initial hot carrier energy distributions due to interband transitions in (a) aluminum, (b) silver, (c) copper, and (d) gold as predicted using detailed electronic structure methods [66]. The top panels annotate the allowed interband transitions on the electronic band structure of each metal. The position of the *d* bands relative to the Fermi level produces hotter holes than electrons in copper and gold, compared to hot holes and electrons in silver, and nearly uniform energy distributions of electrons and holes in aluminum. The bottom panels show that the energy–momentum distribution of hot carriers, plotted with energy on radial axis and direction set by momentum, is highly anisotropic and, for the noble metals, is determined by crystal directions rather than polarization. Adapted with permission from Ref. 66 (© 2014 Nature Publishing Group).

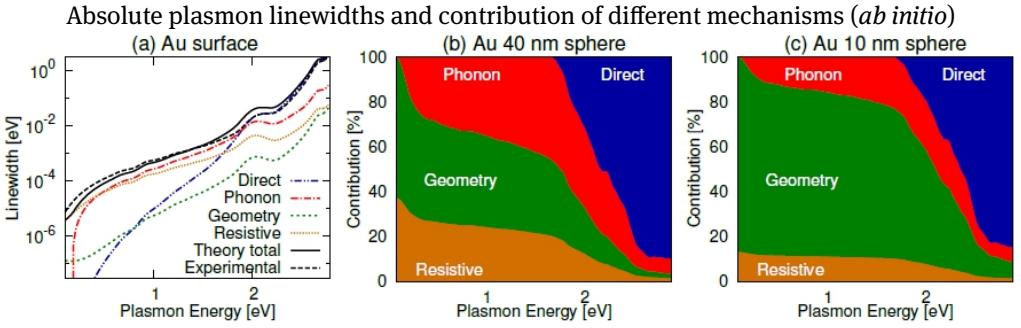

Fig. 5. Absolute linewidths estimated from measured complex dielectric functions compared to theoretical predictions [67] including contributions from resistive losses, direct, geometry-assisted and phonon-assisted transitions for (a) surface plasmon polaritons, and relative contributions of these mechanisms in (b) 40 nm and (c) 20 nm Au spheres. The geometry-assisted contributions are negligible for the surface plasmon, comparable to the phonon-assisted and resistive contributions below threshold for the 40 nm sphere and increase with decreasing particle size, but direct transitions always dominate above the interband threshold energy. Adapted with permission from Ref. 67 (© 2015 American Chemical Society).

tions can therefore guide material and nanostructure design for applications that require carriers of specific polarity and energy.

3 Transport of plasmonic hot carriers

The decay of surface plasmons generates hot carriers through several mechanisms including direct interband transitions, phonon-assisted intraband transitions,

and geometry-assisted intraband transitions, as discussed above. These carriers can be generated with finite probability anywhere inside the plasmonic metal with a distribution of initial momenta, and travel through the material scattering against electrons, phonons, and defects in the metal. These scattering events thermalize the carriers and bring their energies closer to the Fermi level of the metal, on average. Plasmonic hot carrier applications, on the other hand, require carriers far from the Fermi level to more efficiently drive reactions in molecules or cross-Schottky barriers into semiconductor bands. The challenge in designing efficient plasmonic hot carrier devices is, therefore, to collect the hot carriers at the surface of the plasmonic nanostructure with minimal scattering.

Charge carrier transport is of critical importance in several fields, including traditional semiconductors [71] and low-dimensional materials [72]. The transport is usually analyzed in one of two regimes: ballistic, where the carriers rarely scatter within the characteristic structure dimensions, and diffusive, where the carriers scatter several times on length scales much smaller than the structure. Ballistic transport in low-dimensional systems is often treated as a quantum mechanical transmission problem, such as within Landauer theory [73, 74]. Diffusive transport often involves small perturbations from equilibrium that can be described using spatially varying quasi-Fermi-levels, such as the drift-diffusion model for semiconductors [71].

The general case – structures that are neither much smaller nor much larger than the mean free path between carrier scattering events – falls between the ballistic and diffusive regimes. This intermediate regime can be treated using the Boltzmann equation that evolves phase space (momentum and spatial) distribution functions [75] or using Monte Carlo methods [76], but these are computationally feasible only in special (high-symmetry) limits or with approximate simplifications tailored for the specific problem. Plasmonic hot carrier devices often belong to this intermediate regime, as we discuss below, and the goals explicitly require carriers far from equilibrium, which makes analyzing the carrier transport particularly challenging.

The full description of non-equilibrium carrier transport involves several variables: the spatial and temporal evolution of energy and momentum distributions of the hot carriers. We examine plasmonic hot carrier dynamics from two orthogonal simpler perspectives: ultrafast dynamics in pump–probe measurements, where spatial dependence is usually unimportant [77], and the steady-state transport in nanostructures at continuous-wave illumination, where time dependence is not important. The former is more convenient for (indirectly) probing the carrier dynamics experimentally, whereas the latter is relevant for plasmonic energy conversion devices.

3.1 Hot carrier dynamics: ultrafast and fast timescales

Ultrafast pump–probe measurements of plasmonic nanostructures use a high-intensity laser pulse to excite a large number of electrons and measure the optical response as a function of time using a delayed probe pulse [77, 78]. The typical signal observed in these experiments is an initial fast rise (10–100 fs) attributed to electron–electron scattering that converts fewer high-energy excited carriers into several more lower-energy carriers, followed by a slower decay (100 fs to 1 ps) attributed to electron–phonon scattering.

Figure 1 schematically shows the typical electron distributions as a function of time in such experiments. This is phenomenologically described by a "two-temperature model" that tracks the time dependence (and optionally also spatial variation) of separate electron and lattice temperatures, T_e and T_l respectively. The initial excitation generates an electron distribution that is far from equilibrium for which temperature is not well-defined.

Electron–electron scattering equilibrates the electrons with each other in $\sim$ 100 fs, with a typical mean-free-time between collisions for each electron ranging from $\sim$ 10 fs to $\sim$ 100 fs depending on the energy of the electron relative to the Fermi level. Figure 6(a) shows *ab initio* calculations of the electron–electron scattering lifetime of electrons in gold [79]. As expected from Fermi liquid theory, the phase space for collisions increases quadratically with energy difference from the Fermi level, and the lifetime drops approximately as $(E - E_f)^{-2}$. Electron-defect scattering also contributes in polycrystalline metal structures, but electron–electron scattering dominates for high-energy carriers due to the quadratically increasing phase space. At times $\gtrsim$ 100 fs, the electrons can be described approximately by an elevated electron temperature T_e, and the subsequent dynamics can be adequately described within the two-temperature model.

Electron–phonon scattering in the noble metals and other plasmonic metals such as aluminum occurs with a mean-free-time $\sim$10–30 fs, but the energy transferred in each collision is limited by their small Debye energies $\sim$0.02–0.04 eV compared to the typical excitation energies of $\sim$1–3 eV. Therefore, in spite of electron–phonon collisions occurring at approximately the same rate as electron–electron collisions, the net energy transfer occurs $\sim$ 100 times slower resulting in the observed slower

equilibration of electrons with the lattice at picosecond timescales.

The two-temperature model can be used to extract phenomenological estimates of electron and phonon coupling strengths and relaxation times from experiment, or these parameters can be calculated *ab initio* [80, 81]. Deviations due to overlap of electron thermalization and electron–phonon equilibration time scales can also be dealt with phenomenologically [82] or calculated using spatially independent jellium Boltzmann equation approaches [83] However, most of the detailed information currently available from these approaches deals with partially or fully thermalized electrons, which is "too late" for the efficient use of plasmonic hot carriers for energy conversion. Extensions of the two-temperature model that account for non-thermal electrons as an additional energy source for the thermalized electrons and phonons [84] make it possible to analyze the effect of these non-thermal electrons on photocatalysis at metal surfaces [85]. We focus next on using scattering rates derived from theory, and corroborated by experiment in certain regimes, to understand the spatial dependence of hot carrier transport and its implications for device design.

3.2 Spatial dependence of hot carrier distributions

The effect of carrier scattering on the efficiency of plasmonic hot carrier devices has been estimated approximately using different approaches. The simplest approach is to incorporate the lifetime τ of the carriers directly in the calculation of the carrier generation as a Lorentzian broadening $\hbar\tau^{-1}$ of the energy conservation in Fermi's golden rule [64], which results in the predictions shown in Figure 3(b) for τ ranging from 50 fs to 1 ps in nanoparticles of different sizes. However, this approach ignores the strong energy dependence of the electron lifetime due to electron–electron scattering (Figure 6(a)), and the spatial dependence of the carrier distributions due to transport. Additionally, the assumed constant lifetimes are much longer than the practical values for the hot electrons with energies ∼1–3 eV.

Exponential attenuation models $\exp(-L/\lambda)$ based on a fixed mean free path λ may also be used to estimate carrier collection [86]. These approaches also usually neglect the tremendous variation in carrier mean free path with energy. Further, all these approaches neglect the carriers that are generated from the scattering of the initially excited carriers. *Ab initio* calculations of electron–electron scattering [79] indicate that the energy transferred by a hot electron is uniformly distributed between zero and its energy relative to the Fermi level (Figure 6(b)), in agreement with phase-space arguments from Fermi liquid theory. Therefore, secondary electrons (after scattering once) can also carry energy comparable to the primary electrons, and it is important to account for the evolution of carrier energy distributions through the first few scattering events at least.

A full analysis of the transport of plasmonic hot carriers that correctly accounts for all of these effects requires treatment using the Boltzmann equation with spatial dependence. This analysis would be highly desirable for understanding the efficiency of plasmonic energy conversion, but it would be computationally challenging and does not seem to have been performed as yet.

To gain some insight into the complex strongly energy-dependent transport of plasmonic hot carriers, we present a simplified version of the Boltzmann analysis that captures the essential features. We solve the time-dependent spatially–homogeneous Boltzmann equation, and infer the dependence on the transport distance L from the time dependence using

$$v\frac{\mathrm{d}f}{\mathrm{d}L} = \Gamma[f], \tag{1}$$

where v is the carrier velocity, f is the energy and momentum probability distribution, and Γ is the collision integral calculated using Fermi's golden rule for electron–electron and electron–phonon scattering that implicitly includes the strong energy dependence of carrier lifetimes.

Figure 6(c) shows the evolution of energy and momentum distribution of carriers in gold with transport distance, starting from plasmonic excitation at $\hbar\omega$ = 2.6 eV. The initial carrier distribution is dominated by direct transitions, consists of high-energy holes and lower energy electrons, and is strongly anisotropic constrained to crystal directions [66]. The high energy holes are extremely short-lived and scatter significantly even at the small transport distance of L = 3 nm, where the lower energy electrons are still mostly unscattered. By L = 10 nm, the holes have a continuous energy distribution from zero to the plasmon energy, and by L = 30 nm, both electrons and holes are predominantly within 1 eV of the Fermi level. The electron and hole distributions thermalize with each other and become symmetric by L = 100 nm. The initial anisotropy in the momentum distribution also disappears within this transport distance.

Hot carrier transport establishes the link between the electromagnetic field profiles, which determine hot carrier generation and the spatial dependence of carrier collection. The strong dependence of electron–electron scattering rates on energy implies vastly different length scales

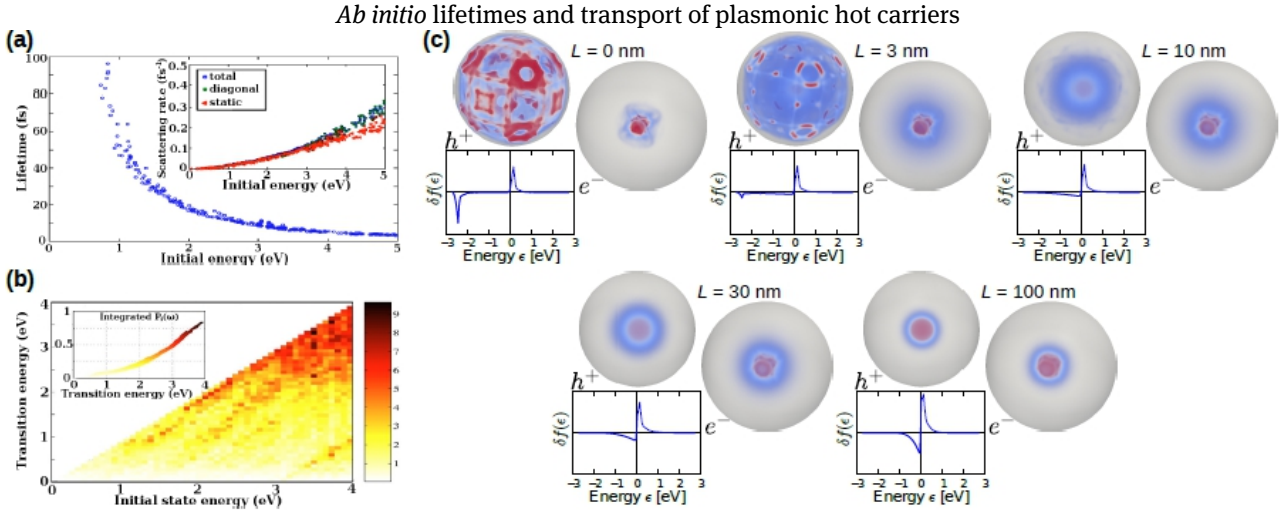

Fig. 6. (a) *Ab initio* calculations of electron–electron scattering show that the carrier scattering rates depend strongly on carrier energy – approximately quadratically with energy relative to Fermi level, and (b) that each scattering event transfers energy with an almost uniform distribution [79]. Note that the maximum lifetime of carriers > 1 eV is less than the smallest constant lifetime $\tau = 0.05$ ps assumed for the jellium estimates in Fig. 3(b). (c) The energy–momentum distribution of hot carriers evolves with transport distance L due to electron–electron and electron–phonon scattering, starting from a strongly anisotropic distribution with hotter holes than electrons (as in Fig. 4(d)). The holes relax to energies $\sim$ 1 eV within $L = 10$ nm, and the distribution becomes isotropic and symmetric between electrons and holes within $L = 100$ nm. Parts (a, b) adapted with permission from Ref. 79 (© 2004 American Physical Society).

depending on the carrier energy: 1 eV electrons in gold may be collected efficiently 100 nm away, whereas 2 eV holes must be collected within 10 nm from where they are generated. Detailed computational modeling of hot carrier transport that fully accounts for these material-dependent effects simultaneously with the geometry of plasmonic nanostructures, the electromagnetic field, and carrier generation profiles is therefore highly desirable.

4 Collection and injection of plasmonic hot carriers in devices

The carriers generated by plasmon decay impinge upon the surface of a plasmonic nanostructure, either directly or after scattering against other carriers and phonons in the metal. Combining theoretical calculations for carrier generation with a transport simulation should be able to predict the energy and spatial distribution of this carrier flux. The final step, as illustrated in Fig. 2, is the injection of the carriers into molecules to drive chemical reactions or their collection in a semiconductor. In this section, we review the considerations for efficient molecular and solid-state collection, as well as the promising alternative of directly generating carriers across a metal–semiconductor interface.

We discuss the collection efficiency of electrons and holes separately for simplicity, but both carriers must be collected in a practical device. For example, if electrons are collected more efficiently than holes, the plasmonic structure will develop a charge imbalance, building up a potential that opposes the electron collection until a steady state is reached where both carriers are collected equally. Therefore, the net collection efficiency of a hot carrier device will be limited by the smaller of the electron and hole collection efficiencies.

4.1 Solid-state collection

The collection of photo-excited hot carriers over a metal–semiconductor Schottky junction, has been studied extensively and is well-described by the Fowler theory for internal photoemission [90] and its refinements [91]. The Fowler yield estimate results from a semiclassical model of electrons overcoming an energy barrier, as shown in Fig. 7(a, b) [87]. Carriers with energy less than the barrier height are reflected. For carriers that cross the barrier, only the normal component of the momentum changes at the interface, which implies that the tangential momentum must be small enough that its kinetic energy contribution in the semiconductor must be less than the excess energy over the barrier; carriers with greater tangential momentum will be reflected (analogous to total internal

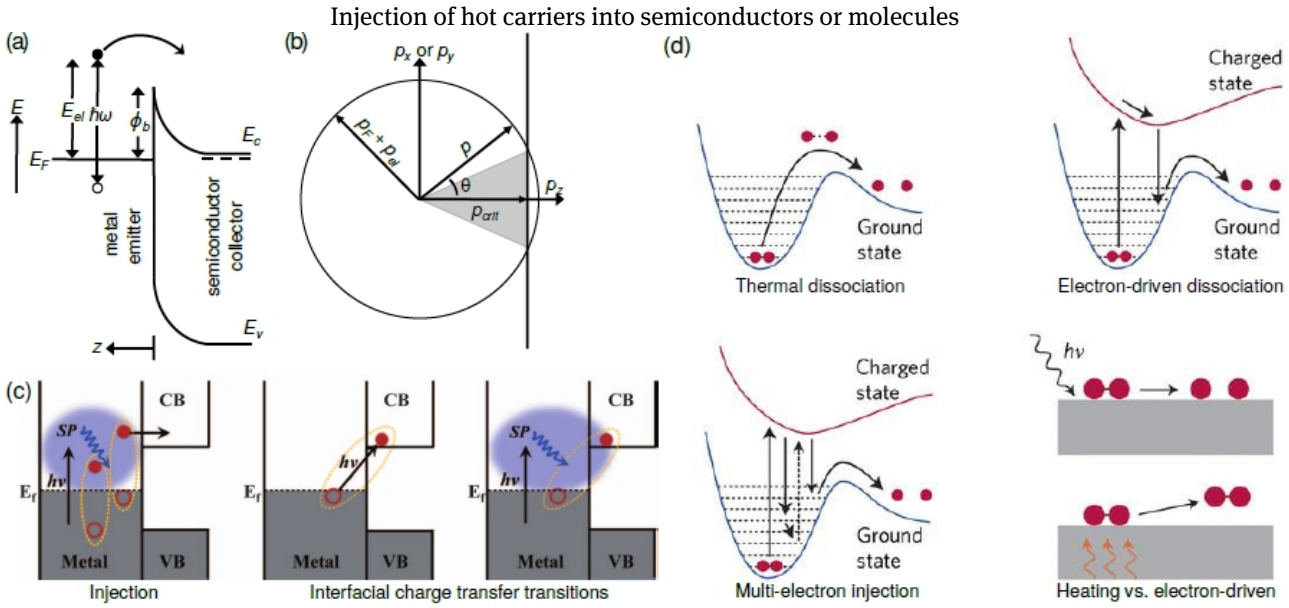

Fig. 7. (a) Energy and (b) momentum-matching considerations for carrier injection through a metal–semiconductor Schottky junction: carrier energy must exceed the Schottky barrier and its incidence angle must lie within an "escape cone" [87]. (c) Carrier collection in semiconductors can occur via plasmon decay in the metal followed by injection or directly by exciting interfacial charge-transfer transitions that generate carriers in the semiconductor [88]. (d) Injection of plasmonic hot carriers can push a molecule into a charged anti-bonding state to induce bond dissociation, in contrast to dissociation via thermal activation [89]. Parts (a, b) adapted with permission from Ref. [87] (© 2014 AIP Publishing), (c) from Ref. 88 (© 2015 AAAS), and (d) from Ref. 89 (© 2015 Nature Publishing Group).

reflection of light). Therefore, only carriers in an "escape cone" around normal incidence cross the barrier, and the angle of this cone increases with carrier energy starting from zero for carriers with the threshold energy to cross the barrier. This results in a quadratic dependence of the injection rate with energy above threshold.

The collection of plasmonic hot carriers has been demonstrated in insulators as well as semiconductors, and the built-in electric fields in the Schottky junction assist in the collection of the emitted hot carriers [28, 92, 93]. Fowler theory remains qualitatively valid regardless of the band structure of the semiconductor or insulator [94, 95], but the magnitudes can differ substantially for materials with high density-of-states near the band edges, such as transition metal oxides. In this case, the shallow electron dispersion relation (localized states) that causes the high density of states makes the escape cones narrower reducing the efficiency of injection. Experimentally, roughened surfaces can overcome these restrictions by providing tangential momentum for the carrier injection [86]. Another opportunity for plasmonic hot carriers in context of solid state systems is to modify the photoluminescence from wide band gap semiconductors or for up-conversion in semiconductor quantum wells.

4.2 Molecular injection: plasmon-enhanced catalysis and femtochemistry

Hot carriers generated by plasmon decay can also inject directly into molecules adsorbed at the surface, directly driving chemical reactions for photochemical energy conversion. Surface photochemistry, chemical reactions driven by photoexcited carriers at metal surfaces, has been well studied in many contexts including solar energy conversion and atmospheric chemistry [37, 96–98]. The possibility of efficiently absorbing light and generating hot carriers in metal nanostructures using plasmon resonances has driven a lot of research in plasmon-driven photocatalysis [33, 45, 99–103]. In particular, "semiconductor-free" water-splitting devices using only plasmonic hot carriers have been demonstrated recently [45].

Understanding mechanisms of chemical reactions driven by hot carriers is an important direction for further advancing plasmonic photochemistry. The most detailed experimental probes of such mechanisms are pump–probe measurements, where two laser pulses with a variable delay are used to excite electronic transitions in a molecule and then probe the progress of the chemical reaction that ensues on femtosecond timescales. In the field of femtochemistry, such techniques have been invaluable for tracking reaction mechanisms or even for changing the

branching ratios of different processes [104–115]. These techniques are now becoming useful to probe the highly non-equilibrium processes driven by plasmonic hot carriers [36, 39, 116].

The basic proposed mechanism for plasmon-driven chemistry involves the injection of an electron from the metal into an anti-bonding state of an adsorbed molecule, causing either desorption or the dissociation of a bond in the adsorbate [117, 118]. Variants of this mechanism can explain the observed chemical activity of various metal nanostructures, as discussed in detail in a recent review article [89]. The adsorbate forms a transient ion strongly coupled to the plasmonic particle, and the relevant potential energy surface is that of an excited state of the adsorbate–plasmonic particle complex, which must be treated together. Theoretical calculations of the excited-state energy landscape using first-principles beyond-ground-state electronic structure methods are therefore essential for predicting such mechanisms and for interpreting femtochemistry experiments [119–121].

A second class of possible mechanisms involves plasmonic enhancement of transitions between states localized on the adsorbate [37, 96]. Here, the involved excited states are primarily those of the adsorbate, and the metal nanostructure serves to enhance the matrix element for the transition by plasmonic enhancement of the surface electric field. Both types of mechanisms require low-lying molecular orbitals on the adsorbate, but the second class does not rely on alignment of adsorbate levels with those of the metal or on hot carrier transport in the metal. These neutral-adsorbate mechanisms will therefore play an important role in future applications of high-efficiency plasmonic catalysis.

Finally, efficient light capture in plasmonic nanostructures can also cause significant local heating and enhance the rates of thermal reactions (not driven by photocarriers) [34]. Photo-thermal reaction enhancement has been demonstrated experimentally though explicit calculations of these processes has also been elusive [34, 122–124].

4.3 Interface science for plasmonic hot carriers

Traditionally, semiconductor–semiconductor heterostructures, hot carriers and photosensitizers (dye sensitizers for example) have been used to expand the range over which absorption can occur but band alignment and interfacial charge-transfer issues limit the realizable enhancement. This has also been a challenge for plasmonic hot carrier injection into semiconductors with unfavorable band alignment. Recent work has demonstrated a direct, instantaneous transfer of plasmon-derived electrons into interfacial semiconductors called plasmon-induced interfacial charge-transfer transition. The mechanism here is via the decay of a plasmon that directly excites an electron from the metal to a strongly coupled acceptor. Such an interfacial charge transfer could have very high quantum efficiencies (highest demonstrated so far has been 24 percent) [88]. Similarly in molecular systems, chemical damping at the interface can involve a direct charge-transfer mechanism where excited carriers are directly injected into an adsorbate acceptor state without first occupying available states in the metal [101, 125–128]. Interface damping, solid-state and molecular, present unique opportunities for high-efficiency plasmonic hot carrier injection and collection and require further experimental and theoretical investigation for a complete understanding of their underlying mechanisms and fundamental limits.

5 Outlook

Splitting plasmonic hot carrier driven processes into steps: plasmon excitation, hot carrier generation, carrier transport and collection, allows building a complete microscopic picture with different levels of theory appropriate for each step. The vast majority of theoretical investigations focus on plasmon excitation (optical response) and hot carrier generation, while fewer studies deal with carrier collection and transport. Here, we conclude with a short discussion of open directions and unanswered questions that future work in plasmonic hot carrier devices should address.

Hot carriers generated by plasmon decay are limited by the photon energy. A given energy-conversion process is usually associated with a characteristic energy, for example, semiconductor band gap in photovoltaics, such that lower-energy photons are incapable of driving the process, while the excess energy of higher-energy photons is wasted. The efficiency of solar energy conversion could be improved by harvesting the energy of these higher and lower energy photons, by producing multiple electron–hole pairs (down-conversion) or single electron–hole pairs from multiple photons (up-conversion). Sub-band-gap injection from plasmonic metals to semiconductors can be used to achieve up-conversion, whereas careful design in geometry to optimize for a single electron–electron scattering event could, in principle achieve, the generation of

two electron–hole pairs, analogous in effect to multiple exciton generation in semiconductors.

The design of hot carrier devices that carefully optimize against or even exploit carrier scattering require developments in theoretical and computational methods that account for nonequilibrium transport in greater detail. As we discussed in Section 3, these methods should be able to account for a few scattering events, at least, while retaining energy, momentum, and spatial dependence, perhaps using an appropriate yet practicable limit of the Boltzmann equation. Extension to nonlinear perturbations additionally including time dependence will be necessary to provide a link between femtosecond pump–probe measurements and the typically low-intensity steady-state regime of plasmonic energy conversion. Detailed analysis of scattering mechanisms and transport can also provide insight into designing new materials, which are suitable for carrier transport, especially with doped-semiconductor plasmonic materials where electronic band structures, and hence phase-space for generation as well as scattering, could be controlled by altering composition.

The final link between hot carrier generation and the energy conversion process is the collection or injection mechanism. Understanding mechanisms and kinetics of chemical reactions driven by hot carriers that are far from equilibrium requires further development of theoretical methods [89]. Direct plasmonic hot carrier generation in semiconductors via interfacial charge-transfer excitations [88] is a particularly exciting direction that could eliminate bottlenecks due to carrier transport, but requires further analysis of its contribution relative to generation in the metal followed by injection in order to guide the design of optimum interfaces.

As the fields of quantum plasmonics and quantum optics merge with electronic structure theory, there are many questions about the fundamental nature of plasmons to be answered, including a many-body understanding of plasmons in the dispersive regime. While there have been demonstrations of the quantum behavior of plasmons, being close to light-line has limited the insight we obtain of the quantum nature of "lossy" plasmons.

Acknowledgment: This material is based upon work performed by the Joint Center for Artificial Photosynthesis, a DOE Energy Innovation Hub, supported through the Office of Science of the U.S. Department of Energy under Award Number DE-SC0004993. P. N. is supported by a National Science Foundation Graduate Research Fellowship and by the Resnick Sustainability Institute.

References

[1] John Pendry. Playing tricks with light. *Science*, 285(5434):1687–1688, 09 1999.

[2] William L. Barnes, Alain Dereux, and Thomas W. Ebbesen. Surface plasmon subwavelength optics. *Nature*, 424(6950):824–830, 08 2003.

[3] Jon A. Schuller, Edward S. Barnard, Wenshan Cai, Young Chul Jun, Justin S. White, and Mark L. Brongersma. Plasmonics for extreme light concentration and manipulation. *Nat Mater*, 9(3):193–204, 03 2010.

[4] Stefan Alexander Maier. *Plasmonics: fundamentals and applications*. Springer Science and Business Media, 2007.

[5] E. Altewischer, M. P. van Exter, and J. P. Woerdman. Plasmon-assisted transmission of entangled photons. *Nature*, 418(6895):304–306, 07 2002.

[6] Dmitri K. Gramotnev and Sergey I. Bozhevolnyi. Plasmonics beyond the diffraction limit. *Nat Photon*, 4(2):83–91, 02 2010.

[7] D. E. Chang, A. S. Sørensen, P. R. Hemmer, and M. D. Lukin. Quantum optics with surface plasmons. *Phys. Rev. Lett.*, 97:053002, Aug 2006.

[8] A. V. Akimov, A. Mukherjee, C. L. Yu, D. E. Chang, A. S. Zibrov, P. R. Hemmer, H. Park, and M. D. Lukin. Generation of single optical plasmons in metallic nanowires coupled to quantum dots. *Nature*, 450(7168):402–406, 11 2007.

[9] Darrick E. Chang, Anders S. Sorensen, Eugene A. Demler, and Mikhail D. Lukin. A single-photon transistor using nanoscale surface plasmons. *Nat Phys*, 3(11):807–812, 11 2007.

[10] D.C. Marinica, A.K. Kazansky, P. Nordlander, J. Aizpurua, and A. G. Borisov. Quantum plasmonics: Nonlinear effects in the field enhancement of a plasmonic nanoparticle dimer. *Nano Letters*, 12(3):1333–1339, 2012.

[11] Y. Fedutik, V. V. Temnov, O. Schöps, U. Woggon, and M. V. Artemyev. Exciton-plasmon-photon conversion in plasmonic nanostructures. *Physical Review Letters*, 99(13):136802–, 09 2007.

[12] Z. Fang. Graphene-antenna sandwich photodetector. *Nano Lett.*, 12:3808–3813, 2012.

[13] Zheyu Fang, Yumin Wang, Zheng Liu, Andrea Schlather, Pulickel M. Ajayan, Frank H. L. Koppens, Peter Nordlander, and Naomi J. Halas. Plasmon-induced doping of graphene. *ACS Nano*, 6(11):10222–10228, 2014/08/28 2012.

[14] Vincenzo Giannini, Antonio I. Fernández-Domínguez, Susannah C. Heck, and Stefan A. Maier. Plasmonic nanoantennas: Fundamentals and their use in controlling the radiative properties of nanoemitters. *Chemical Reviews*, 111(6):3888–3912, 2014/08/28 2011.

[15] H. Chalabi, D. Schoen, and M. Brongersma. Hot-electron photodetection with a plasmonic nanostripe antenna. *Nano Lett.*, 14:1374–1380, 2014.

[16] Harry A. Atwater and Albert Polman. Plasmonics for improved photovoltaic devices. *Nat Mater*, 9(3):205–213, 03 2010.

[17] Eric W. McFarland and Jing Tang. A photovoltaic device structure based on internal electron emission. *Nature*, 421(6923):616–618, 02 2003.

[18] Giuliana Di Martino, Yannick Sonnefraud, Stéphane Kéna-Cohen, Mark Tame, Şahin K. Özdemir, M. S. Kim, and Stefan A. Maier. Quantum statistics of surface plasmon polari-

tons in metallic stripe waveguides. *Nano Letters*, 12(5):2504–2508, 2014/10/20 2012.

[19] G. Di Martino, Y. Sonnefraud, M. S. Tame, S. Kéna-Cohen, F. Dieleman, Ş. K. Özdemir, M. S. Kim, and S. A. Maier. Observation of quantum interference in the plasmonic hong-ou-mandel effect. *Phys. Rev. Applied*, 1:034004, Apr 2014.

[20] James S. Fakonas, Hyunseok Lee, Yousif A. Kelaita, and Harry A. Atwater. Two-plasmon quantum interference. *Nat Photon*, 8(4):317–320, 04 2014.

[21] M. S. Tame, K. R. McEnery, S. K. Ozdemir, J. Lee, S. A. Maier, and M. S. Kim. Quantum plasmonics. *Nat Phys*, 9(6):329–340, 06 2013.

[22] M. S. Tame, C. Lee, J. Lee, D. Ballester, M. Paternostro, A. V. Zayats, and M. S. Kim. Single-photon excitation of surface plasmon polaritons. *Physical Review Letters*, 101(19):190504–, 11 2008.

[23] D. Ballester, M. S. Tame, C. Lee, J. Lee, and M. S. Kim. Long-range surface-plasmon-polariton excitation at the quantum level. *Physical Review A*, 79(5):053845–, 05 2009.

[24] S. Kuhn, U. Hakanson, L. Rogobete, and V. Sandoghdar. Enhancement of single-molecule fluorescence using a gold nanoparticle as an optical nanoantenna. *Phys. Rev. Lett.*, 97:017402, 2006.

[25] Pascal Anger, Palash Bharadwaj, and Lukas Novotny. Enhancement and quenching of single-molecule fluorescence. *Phys. Rev. Lett.*, 96:113002, Mar 2006.

[26] R. D. Artuso and G. W. Bryant. Strongly coupled quantum dot–metal nanoparticle systems: exciton-induced transparency, discontinuous response, and suppression as driven quantum oscillator effects. *Phys. Rev. B*, 82:195419, 2010.

[27] Shaunak Mukherjee, Florian Libisch, Nicolas Large, Oara Neumann, Lisa V. Brown, Jin Cheng, J. Britt Lassiter, Emily A. Carter, Peter Nordlander, and Naomi J. Halas. Hot electrons do the impossible: Plasmon-induced dissociation of h2 on au. *Nano Letters*, 13(1):240–247, 2013/07/23 2012.

[28] Yukina Takahashi and Tetsu Tatsuma. Solid state photovoltaic cells based on localized surface plasmon-induced charge separation. *Applied Physics Letters*, 99(18):182110–3, 10 2011.

[29] Fuming Wang and Nicholas A. Melosh. Plasmonic energy collection through hot carrier extraction. *Nano Letters*, 11(12):5426–5430, 2013/07/23 2011.

[30] P. James Schuck. Nanoimaging: Hot electrons go through the barrier. *Nat Nano*, 8(11):799–800, 11 2013.

[31] Syed Mubeen, Joun Lee, Nirala Singh, Stephan Kramer, Galen D. Stucky, and Martin Moskovits. An autonomous photosynthetic device in which all charge carriers derive from surface plasmons. *Nat Nano*, 8(4):247–251, 04 2013.

[32] Suljo Linic, Phillip Christopher, and David B. Ingram. Plasmonic-metal nanostructures for efficient conversion of solar to chemical energy. *Nat Mater*, 10(12):911–921, 12 2011.

[33] S. Mubeen, G. Hernandez-Sosa, D. Moses, J. Lee, and M. Moskovits. Plasmonic photosensitization of a wide band gap semiconductor: converting plasmons to charge carriers. *Nano Lett.*, 11:5548–5552, 2011.

[34] J. Adleman, D. Boyd, D. Goodwin, and D. Psaltis. Heterogenous catalysis mediated by plasmon heating. *Nano Lett.*, 9:4417–4423, 2009.

[35] K. Awazu. Plasmonic photocatalyst consisting of silver nanoparticles embedded in titanium dioxide. *J. Am. Chem. Soc.*, 130:1676–1680, 2008.

[36] L. Brus. Noble metal nanocrystals: Plasmon electron transfer photochemistry and single-molecule raman spectroscopy. *Acc. Chem. Res.*, 41:1742–1749, 2008.

[37] S. Buntin, L. Richter, R. Cavanagh, and D. King. Optically driven surface reactions: Evidence for the role of hot electrons. *Phys. Rev. Lett.*, 61:1321–1324, 1988.

[38] P. Christopher, D. B. Ingram, and S. Linic. Enhancing photochemical activity of semiconductor nanoparticles with optically active ag nanostructures: Photochemistry mediated by ag surface plasmons. *J. Phys. Chem. C*, 19:9173–9177, 2010.

[39] P. Christopher, H. Xin, and S. Linic. Visible light enhanced catalytic oxidation reactions on plasmonic ag nanostructures. *Nature Chem.*, 3:467–472, 2011.

[40] J-J. Chen, J. C. S. Wu, P. C. Wu, and D. P. Tsai. Plasmonic photocatalyst for h2 evolution in photocatalytic water splitting. *J. Phys. Chem. C*, 115:210–216, 2011.

[41] S. K. Cushing. Photocatalytic activity enhanced by plasmonic resonant energy transfer from metal to semiconductor. *J. Am. Chem. Soc*, 134:15033–15041, 2012.

[42] S. K. Cushing and N. Q. Wu. Plasmon-enhanced solar energy harvesting. *Interface*, 22:63–67, 2013.

[43] C. Frischkorn and M. Wolf. Femtochemistry at metal surfaces: Nonadiabatic reaction dynamics. *Chem. Rev.*, 106:4207–4233, 2006.

[44] Cesar Clavero. Plasmon-induced hot-electron generation at nanoparticle/metal-oxide interfaces for photovoltaic and photocatalytic devices. *Nat Photon*, 8(2):95–103, 02 2014.

[45] Martin Moskovits. The case for plasmon-derived hot carrier devices. *Nat Nano*, 10(1):6–8, 01 2015.

[46] Mark L. Brongersma, Naomi J. Halas, and Peter Nordlander. Plasmon-induced hot carrier science and technology. *Nat Nano*, 10(1):25–34, 01 2015.

[47] Viktoriia E. Babicheva, Sergei V. Zhukovsky, Renat Sh. Ikhsanov, Igor E. Protsenko, Igor V. Smetanin, and Alexander Uskov. Hot electron photoemission from plasmonic nanostructures: The role of surface photoemission and transition absorption. *ACS Photonics*, 07 2015.

[48] Hui Zhang and Alexander O. Govorov. Optical generation of hot plasmonic carriers in metal nanocrystals: The effects of shape and field enhancement. *The Journal of Physical Chemistry C*, 118(14):7606–7614, 2014.

[49] Bob Y. Zheng, Hangqi Zhao, Alejandro Manjavacas, Michael McClain, Peter Nordlander, and Naomi J. Halas. Distinguishing between plasmon-induced and photoexcited carriers in a device geometry. *Nat Commun*, 6, 07 2015.

[50] Zubin Jacob and Vladimir M. Shalaev. Plasmonics goes quantum. *Science*, 334(6055):463–464, 10 2011.

[51] Denis Jacquemin, Benedetta Mennucci, and Carlo Adamo. Excited-state calculations with td-dft: from benchmarks to simulations in complex environments. *Physical Chemistry Chemical Physics*, 13(38):16987–16998, 2011.

[52] J D Whitfield, M-H Yung, D G Tempel, S Boixo, and A Aspuru-Guzik. Computational complexity of time-dependent density functional theory. *New Journal of Physics*, 16(8):083035, 2014.

[53] P. Song, P. Nordlander, and S. Gao. Quantum mechanical study of the coupling of plasmon excitations to atomic-scale electron transport. *J Chem Phys*, 134(7):074701, Feb 2011.

[54] J. Zuloaga, E. Prodan, and P. Nordlander. Quantum description of the plasmon resonances of a nanoparticle dimer. *Nano Lett.*, 9(2):887–891, Feb 2009.

[55] A. Manjavacas, F. J. Garcia de Abajo, and P. Nordlander. Quantum plexcitonics: strongly interacting plasmons and excitons. *Nano Lett.*, 11(6):2318–2323, Jun 2011.

[56] Ruben Esteban, Andrei G. Borisov, Peter Nordlander, and Javier Aizpurua. Bridging quantum and classical plasmonics with a quantum-corrected model. *Nat Commun*, 3:825, 05 2012.

[57] Jun Yan, Karsten W. Jacobsen, and Kristian S. Thygesen. Conventional and acoustic surface plasmons on noble metal surfaces: A time-dependent density functional theory study. *Phys. Rev. B*, 86:241404, Dec 2012.

[58] Christine M. Aikens, Shuzhou Li, and George C. Schatz. From discrete electronic states to plasmons: Tddft optical absorption properties of ag n (n = 10, 20, 35, 56, 84, 120) tetrahedral clusters. *The Journal of Physical Chemistry C*, 112(30):11272–11279, 07 2008.

[59] Nicola Durante, Alessandro Fortunelli, Michel Broyer, and Mauro Stener. Optical properties of au nanoclusters from td-dft calculations. *The Journal of Physical Chemistry C*, 115(14):6277–6282, 2013/11/11 2011.

[60] Gyun-Tack Bae and Christine M. Aikens. Time-dependent density functional theory studies of optical properties of au nanoparticles: Octahedra, truncated octahedra, and icosahedra. *The Journal of Physical Chemistry C*, 09 2015.

[61] P. Bharadwaj, B. Deutsch, and L. Novotny. Optical antennas. *Adv. Opt. Photon.*, 1:438–483, 2009.

[62] L. Landau. On the vibration of the electronic plasma. *J. Phys. USSR*, 10, 1946.

[63] Alexander O. Govorov, Hui Zhang, and Yurii K. Gun'ko. Theory of photoinjection of hot plasmonic carriers from metal nanostructures into semiconductors and surface molecules. *The Journal of Physical Chemistry C*, 117(32):16616–16631, 2013/11/11 2013.

[64] Alejandro Manjavacas, Jun G. Liu, Vikram Kulkarni, and Peter Nordlander. Plasmon-induced hot carriers in metallic nanoparticles. *ACS Nano*, 8(8):7630–7638, 2014/08/28 2014.

[65] A. O. Govorov, H. Zhang, H. V. Demir, and Y. K. Gun'ko. Photogeneration of hot plasmonic electrons with metal nanocrystals: Quantum description and potential applications. *Nano Today*, 9:85–101, 2014.

[66] Ravishankar Sundararaman, Prineha Narang, Adam S. Jermyn, William A. Goddard III, and Harry A. Atwater. Theoretical predictions for hot-carrier generation from surface plasmon decay. *Nat. Commun.*, 5:5788, 2014.

[67] Ana M. Brown, Ravishankar Sundararaman, Prineha Narang, III William A. Goddard, and Harry A. Atwater. Nonradiative plasmon decay and hot carrier dynamics: Effects of phonons, surfaces, and geometry. *ACS Nano*, 10:957, 2016.

[68] M. Bernardi, J. Mustafa, J.B. Neaton, and S.G. Louie. Theory and computation of hot carriers generated by surface plasmon polaritons in noble metals. *Nat. Commun.*, In press, 2015.

[69] Jesse Noffsinger, Emmanouil Kioupakis, Chris G. Van de Walle, Steven G. Louie, and Marvin L. Cohen. Phonon-assisted optical absorption in silicon from first principles. *Phys. Rev. Lett.*, 108:167402, Apr 2012.

[70] Emmanouil Kioupakis, Patrick Rinke, André Schleife, Friedhelm Bechstedt, and Chris G. Van de Walle. Free-carrier absorption in nitrides from first principles. *Phys. Rev. B*, 81:241201, Jun 2010.

[71] Carlo Jacoboni. *Theory of Electron Transport in Semiconductors*. Springer Series in Solid-State Sciences. Springer-Verlag Berlin Heidelberg, 2010.

[72] F. Chen and N. J. Tao. Electron transport in single molecules: From benzene to graphene. *Accounts of Chemical Research*, 42(3):429–438, 2009. PMID: 19253984.

[73] R Landauer. Spatial variation of currents and fields due to localized scatterers in metallic conduction. *IBM Journal of Research and Development*, 1(3):223–231, 1957.

[74] A Nitzan and MA Ratner. Electron transport in molecular wire junctions. *SCIENCE*, 300(5624):1384–1389, MAY 30 2003.

[75] *The Boltzmann Equation and Its Applications*. Applied Mathematical Sciences. Springer New York, 1988.

[76] Carlo Jacoboni and Lino Reggiani. The monte carlo method for the solution of charge transport in semiconductors with applications to covalent materials. *Rev. Mod. Phys.*, 55:645–705, Jul 1983.

[77] Gregory V. Hartland. Optical studies of dynamics in noble metal nanostructures. *Chemical Reviews*, 111(6):3858–3887, 06 2011.

[78] Hayk Harutyunyan, Alex B. F. Martinson, Daniel Rosenmann, Larousse Khosravi Khorashad, Lucas V. Besteiro, Alexander O. Govorov, and Gary P. Wiederrecht. Anomalous ultrafast dynamics of hot plasmonic electrons in nanostructures with hot spots. *Nat Nano*, 10(9):770–774, 09 2015.

[79] Florian Ladstädter, Ulrich Hohenester, Peter Puschnig, and Claudia Ambrosch-Draxl. First-principles calculation of hot-electron scattering in metals. *Phys. Rev. B*, 70:235125, Dec 2004.

[80] Zhibin Lin, Leonid V. Zhigilei, and Vittorio Celli. Electron-phonon coupling and electron heat capacity of metals under conditions of strong electron-phonon nonequilibrium. *Phys. Rev. B*, 77:075133, Feb 2008.

[81] A. Brown, R. Sundararaman, P. Narang, W. A. Goddard III, and H. A. Atwater. Ab initio phonon coupling and optical response of hot electrons in plasmonic metals. preprint: arXiv:1602.00625

[82] Ashutosh Giri, John T. Gaskins, Brian M. Foley, Ramez Cheaito, and Patrick E. Hopkins. Experimental evidence of excited electron number density and temperature effects on electron-phonon coupling in gold films. *Journal of Applied Physics*, 117(4):–, 2015.

[83] N. Del Fatti, C. Voisin, M. Achermann, S. Tzortzakis, D. Christofilos, and F. Vallée. Nonequilibrium electron dynamics in noble metals. *Phys. Rev. B*, 61:16956–16966, Jun 2000.

[84] E. Carpene. Ultrafast laser irradiation of metals: Beyond the two-temperature model. *Phys. Rev. B*, 74:024301, Jul 2006.

[85] Talin Avanesian and Phillip Christopher. Adsorbate specificity in hot electron driven photochemistry on catalytic metal surfaces. *The Journal of Physical Chemistry C*, 118(48):28017–28031, 2014.

[86] Hamidreza Chalabi, David Schoen, and Mark L. Brongersma. Hot-electron photodetection with a plasmonic nanostripe antenna. *Nano Letters*, 14(3):1374–1380, 2014. PMID: 24502677.

[87] A. J. Leenheer, P. Narang, N. S. Lewis, and H. A. Atwater. Solar energy conversion via hot electron internal photoemission in metallic nanostructures: efficiency estimates. *J. Appl. Phys.*, 115:134301, 2014.

[88] K. Wu, J. Chen, J. R. McBride, and T. Lian. Efficient hot-electron transfer by a plasmon-induced interfacial charge-transfer transition. *Science*, 349(6248):632–635, 08 2015.

[89] Suljo Linic, Umar Aslam, Calvin Boerigter, and Matthew Morabito. Photochemical transformations on plasmonic metal nanoparticles. *Nat Mater*, 14(6):567–576, 06 2015.

[90] R. H. Fowler. The analysis of photoelectric sensitivity curves for clean metals at various temperatures. *Physical Review*, 38(1):45–56, 07 1931.

[91] V. L. Dalal. Simple model for internal photoemission. *J. Appl. Phys.*, 42:2274–2279, 1971.

[92] Mark W. Knight, Heidar Sobhani, Peter Nordlander, and Naomi J. Halas. Photodetection with active optical antennas. *Science*, 332(6030):702–704, 05 2011.

[93] Mark W. Knight, Yumin Wang, Alexander S. Urban, Ali Sobhani, Bob Y. Zheng, Peter Nordlander, and Naomi J. Halas. Embedding plasmonic nanostructure diodes enhances hot electron emission. *Nano Letters*, 13(4):1687–1692, 2013/07/23 2013.

[94] D. Peters. An infrared detector utilizing internal photoemission. *Proc. IEEE*, 55:704–705, 1967.

[95] A Sobhani. Narrowband photodetection in the near-infrared with a plasmon-induced hot electron device. *Nature Commun.*, 4:1643, 2013.

[96] D. G. Busch and W. Ho. Direct observation of the crossover from single to multiple excitations in femtosecond surface photochemistry. *Phys. Rev. Lett.*, 77:1338–1341, 1996.

[97] Dietrich Menzel and Robert Gomer. Desorption from metal surfaces by low-energy electrons. *The Journal of Chemical Physics*, 41(11):3311–3328, 1964.

[98] D. N. Denzler, C. Frischkorn, C. Hess, M. Wolf, and G. Ertl. Electronic excitation and dynamic promotion of a surface reaction. *Phys. Rev. Lett.*, 91:226102, 2003.

[99] R. A. Wolkow and M. Moskovits. Enhanced photochemistry on silver surfaces. *J. Chem. Phys.*, 87:5858–5869, 1987.

[100] S. Mubeen. An autonomous photosynthetic device in which all charge carriers derive from surface plasmons. *Nature Nanotechnol*, 8:247–251, 2013.

[101] S. Linic, P. Christopher, and D. B. Ingram. Plasmonic-metal nanostructures for efficient conversion of solar to chemical energy. *Nature Mater.*, 10:911–921, 2011.

[102] W. J. Youngblood. Photoassisted overall water splitting in a visible light-absorbing dye-sensitized photoelectrochemical cell. *J. Am. Chem. Soc.*, 131:926–927, 2009.

[103] X. Zhang. Experimental and theoretical investigation of the distance dependence of localized surface plasmon coupled förster resonance energy transfer. *ACS Nano*, 8:1273–1283, 2014.

[104] Takashi Fuse, Toshiaki Fujino, Jeong-Tak Ryu, Mitsuhiro Katayama, and Kenjiro Oura. Electron-stimulated desorption of hydrogen from h/si(001)-1×1 surface studied by time-of-flight elastic recoil detection analysis. *Surface Science*, 420(1):81–86, 1 1999.

[105] J. W. Gadzuk, L. J. Richter, S. A. Buntin, D. S. King, and R. R. Cavanagh. Laser-excited hot-electron induced desorption: A theoretical model applied to no/pt(111). *Surf. Sci.*, 235:317–333, 1990.

[106] J. W. Gadzuk. Hot-electron femtochemistry at surfaces: on the role of multiple electron processes in desorption. *Chem. Phys.*, 251:87–97, 2000.

[107] J-P Gauyacq, A G Borisov, and A K Kazansky. Theoretical study of excited electronic states at surfaces, link with photo-emission and photo-desorption experiments. *Journal of Physics: Conference Series*, 133(1):012009, 2008.

[108] S. R. Hatch, X-Y. Zhu, J. M. White, and A. Campion. Photoinduced pathways to dissociation and desorption of dioxygen on ag(110) and pt(111). *J. Phys Chem.*, 95:1759–1768, 1991.

[109] K. Fukutani and Y. Murata. Photoexcited processes at metal and alloy surfaces: electronic structure and adsorption site. *Surface Science*, 390(1–3):164–173, 11 1997.

[110] P. Avouris and R. E. Walkup. Fundamental mechanisms of desorption and fragmentation induced by electronic transitions at surfaces. *Annu. Rev. Phys. Chem.*, 40:173–206, 1989.

[111] M. Bonn. Phonon- versus electron-mediated desorption and oxidation of co on ru(0001). *Science*, 285:1042–1045, 1999.

[112] W. D. Mieher and W. Ho. Bimolecular surface photochemistry: mechanisms of co oxidation on pt(111) at 85 k. *J. Chem. Phys.*, 99:9279–9295, 1993.

[113] J. A. Misewich, S. Nakabayashi, P. Weigand, M. Wolf, and T. F. Heinz. Anomalous branching ratio in the femtosecond surface chemistry of o2pd(111). *Surface Science*, 363(1–3):204–213, 8 1996.

[114] J. A. Prybyla, T. F. Heinz, J. A. Misewich, M. M. T. Loy, and J. H. Glownia. Desorption induced by femtosecond laser pulses. *Phys. Rev. Lett.*, 64:1537–1540, 1990.

[115] W. Ho. Reactions at metal surfaces induced by femtosecond lasers, tunneling electrons and heating. *J. Phys. Chem.*, 100:13050–13060, 1996.

[116] P. Christopher, H. Xin, A. Marimuthu, and S. Linic. Singular characteristics and unique chemical bond activation mechanisms of photocatalytic reactions on plasmonic nanostructures. *Nature Mater.*, 11:1044–1050, 2012.

[117] T. Olsen, J. Gavnholt, and J. Schiotz. Hot-electron-mediated desorption rates calculated from excited state potential energy surfaces. *Phys. Rev. B*, 79:035403, 2009.

[118] T. Olsen and J. Schiotz. Origin of power laws for reactions at metal surfaces mediated by hot electrons. *Phys. Rev. Lett.*, 103:238301, 2009.

[119] J. Gavnholt, A. Rubio, T. Olsen, K. Thygesen, and J. Schiotz. Hot-electron-assisted femtochemistry at surfaces: A time-dependent density functional theory approach. *Phys. Rev. B*, 79:195405, 2009.

[120] Peter Elliott and Neepa T. Maitra. Propagation of initially excited states in time-dependent density-functional theory. *Phys. Rev. A*, 85:052510, May 2012.

[121] Hideyuki Inouye, Koichiro Tanaka, Ichiro Tanahashi, and Kazuyuki Hirao. Ultrafast dynamics of nonequilibrium electrons in a gold nanoparticle system. *Phys. Rev. B*, 57:11334–11340, May 1998.

[122] G. Baffou, R. Quidant, and C. Girard. Heat generation in plasmonic nanostructures: Influence of morphology. *Appl. Phys. Lett.*, 94:153109, 2009.

[123] G. Baffou, R. Quidant, and F. J. Garcia de Abajo. Nanoscale control of optical heating in complex plasmonic systems. *ACS Nano*, 4:709–716, 2010.

[124] D. Boyer, P. Tamarat, A. Maali, B. Lounis, and M. Orrit. Photothermal imaging of nanometer-sized metal particles among scatterers. *Science*, 297:1160–1163, 2002.

[125] Hrvoje Petek, Miles J. Weida, Hisashi Nagano, and Susumu Ogawa. Real-time observation of adsorbate atom motion above a metal surface. *Science*, 288(5470):1402–1404, 2000.

[126] Hrvoje Petek. Photoexcitation of adsorbates on metal surfaces: One-step or three-step. *The Journal of Chemical Physics*, 137(9), 2012.

[127] Matthew J. Kale, Talin Avanesian, Hongliang Xin, Jun Yan, and Phillip Christopher. Controlling catalytic selectivity on metal nanoparticles by direct photoexcitation of adsorbate–metal bonds. *Nano Letters*, 14(9):5405–5412, 09 2014.

[128] Run Long and Oleg V Prezhdo. Instantaneous generation of charge-separated state on tio2 surface sensitized with plasmonic nanoparticles. *Journal of the American Chemical Society*, 136(11):4343–4354, 03 2014.